American Journal of Pathology, Vol. 162, No. 4, April 2003

Role of CD31/Platelet Endothelial Cell Adhesion Molecule-1 Expression in *in Vitro* and *in Vivo* Growth and Differentiation of Human Breast Cancer Cells

Luisella Righi,*† Silvia Deaglio,*‡ Carla Pecchioni,† Armando Gregorini,§ Alberto L. Horenstein,*‡ Gianni Bussolati,† Anna Sapino,† and Fabio Malavasi*‡

From the Department of Genetics, Biology, and Biochemistry, Laboratory of Immunogenetics, and the Department of Biomedical Sciences and Human Oncology,† University of Torino Medical School, Torino; the Experimental Medicine Research Center,‡ San Giovanni Battista Hospital, Torino; and the Institute of Biology and Genetics,§ University of Ancona Medical School, Ancona, Italy*

Breast ductal carcinoma *in situ* is an intraductal proliferation of malignant epithelial cells that diffuse within the ductal system without stromal invasion. Our finding that a subset of these tumors express CD31/platelet endothelial cell adhesion molecule-1 suggests that breast cancer represents an informative model for studying the involvement of the molecule in the morphogenesis, differentiation, and diffusion of this disease. Transfection of CD31 in MDA-MB-231 cells caused reduction in growth, loss of CD44, and acquisition of a ductal morphology. The same effects were maintained *in vivo*, in which CD31$^+$ tumors grew with *in situ*-like aspects, papillary differentiation, and a secretory phenotype. CD44 was downmodulated, with the CD31$^+$ cells blocked in the G_1 phase. The morphology was highly similar to what was observed in some human CD31$^+$ ductal carcinomas *in situ*. MDA-MB-231 mock cells grew in solid sheets, lacking stromal material, and displaying high levels of CD44 and proliferation. CD31$^+$ cells acquired motility characteristics in *in vitro* assays, a finding confirmed *in vivo* by the diffusion of human tumor cells throughout the normal ducts residual in the murine mammary gland. In conclusion, CD31 expression reverts the undifferentiated morphology and aggressive behavior of MDA-MB-231 cells, indicating its active role in the morphogenesis of breast ductal *in situ* carcinomas. *(Am J Pathol 2003, 162:1163–1174)*

Human CD31/platelet endothelial cell adhesion molecule (PECAM)-1 is a 130-kd cell surface molecule belonging to the immunoglobulin superfamily and expressed by endothelial cells, platelets, monocytes, polymorphonuclear cells, as well as by discrete populations of circulating lymphocytes.[1] CD31 functions as an adhesion receptor molecule, playing a key role in leukocyte trafficking across the endothelial layer.[2,3] A number of reports have indicated that CD31 may engage in homophilic (CD31-CD31) and heterophilic (CD31-X) bindings to other cell surface or matrix proteins. Ligand-receptor binding results in lymphocyte rolling, adhesion, and extravasation, as well as in the implementation of a signaling pathway, partly intertwined with the one controlled by integrins.[4] The proposed counterreceptors for CD31 include the integrin $\alpha_v\beta_3$,[5,6] a molecule present on red blood cells,[7] an as yet unidentified ligand expressed by T cells,[8] and CD38.[9,10]

In addition to its role as an adhesion molecule, recent work has established that CD31 acts as a signaling receptor on leukocytes. Tyrosine and threonine residues in the cytoplasmic tail of CD31 are phosphorylated by Src and PKC family kinases, leading to the recruitment of cytoplasmic signaling and adaptor molecules including the protein tyrosine phosphatases SHP-1 and SHP-2,[11,12] as well as α-catenin[13] and β-catenin.[14] Moreover, CD31 possesses two immunoreceptor tyrosine-based inhibitory motif domains within its cytoplasmic tail.[15,16]

We recently reported on the expression of CD31 by a subset of ductal *in situ* carcinomas (DCIS) of the breast, characterized by high nuclear grade, hormone independence, and a clear propensity to invade the lobules and eventually to give rise to Paget's disease of the nipple.[17] CD31$^+$ DCIS may or may not express CD44, an adhesion molecule involved in tumor metastatization,[18] whereas CD31$^+$ invasive carcinomas are constantly CD44$^+$. These findings suggest that different clones are engaged in invasive growth and intraductal diffusion, although the exact contribution of the two partners remains to be defined.

Supported by the AIRC, Special Projects AIDS (Istituto Superiore di Sanità), Biotechnology (CNR/MURST), and Cofinanziamento (MURST), the Compagnia di San Paolo, Cariverona, and the FIRMS Foundations.

L. R. and S. D. contributed equally to this work.

L.R. is member of a Ph.D. program in Human Oncology; S. D. is a student of the Postgraduate School of Medical Oncology, University of Torino Medical School, Torino, Italy.

Accepted for publication December 30, 2002.

Address reprint requests to Fabio Malavasi, M.D., Laboratory of Immunogenetics, Via Santena, 19, 10126 Torino, Italy. E-mail: fabio.malavasi@unito.it.

The present work provides evidence that CD31 is a cause and not an effect of the events connected with the intraductal modality of tumor growth. Indeed, we show that CD31 is responsible for the acquisition of *in situ*-like features, of papillary differentiation, and of a secretory phenotype by the MDA-MB-231 breast cancer cell line. Moreover, the soundness of this work is confirmed by the transferability of the findings obtained *in vitro* to animal models, with pathological pictures closely reminiscent of those naturally occurring in humans.

Materials and Methods

Cells and Cell Lines

The hormone-independent breast cancer cell line MDA-MB-231[19] and murine L-fibroblasts transfected with the human CD31 cDNA (L-CD31$^+$) or with the empty plasmid (L-mock)[9] were cultured in RPMI 1640 medium (Sigma, Milano, Italy) in the presence of 10% fetal calf serum (Seromed, Berlin, Germany), 100 U/ml penicillin, and 100 μg/ml streptomycin (all from Sigma), hereafter referred to as complete medium. Human umbilical vein endothelial cells were obtained and cultured as detailed elsewhere.[20]

Antibodies

The anti-CD31 monoclonal antibodies (mAbs) included JC70 (DAKO, Glostrup, Denmark), 5F4.9 (from F. Bussolino, Torino, Italy) and Moon-1.[20] Other mAbs used were anti-CD44 (DF1485, DAKO), anti-CD54 (CB-ICAM-1),[21] anti-CD11a (CB11a),[22] anti-CD29 (Moon-4),[9] anti-E-cadherin (H276; Santa Cruz Biotechnology, Santa Cruz, CA), anti-VE-cadherin (F8, Santa Cruz Biotechnology), anti-CD71 (CB26),[23] anti-HLA class I (O1.65),[23] anti-laminin (2233PLA; Euro-Diagnostica, Firenze, Italy), anti-collagen-IV (CIV22, DAKO), anti-human milk fat globule membrane protein (HMFG-2; from J. Taylor-Papadimitriou, London, UK), anti-Ki-67 (MIB-1, DAKO), anti-p27/Kip-1 (11D11; BD Biosciences, Milano, Italy), and anti-p21/WAF/Cip-1 (H164, Santa Cruz Biotechnology).

A fluorescein isothiocyanate-conjugated goat anti-mouse Ig (GαMIg) (Caltag, Burlingame, CA) was used in indirect immunofluorescence studies and a horseradish peroxidase-conjugated GαMIg (Amersham, Cologno Monzese, Italy) was used in Western blot analyses. GαMIgG-coated magnetic beads (Dynal, Oslo, Norway) were used to continuously select CD31$^+$ cells.

Constructs

CD31 cDNA, contained in a pCDM8 plasmid (from H. Stockinger, Vienna, Austria), was amplified by polymerase chain reaction with the primers designed according to the published sequence (GenBank Accession no. M37780). Polymerase chain reaction amplification was performed using an automated DNA thermal cycler (Perkin Elmer, Monza, Italy) for 30 cycles and the reaction product was visualized by electrophoresis.

An aliquot (1 μl) of the polymerase chain reaction product was ligated to a pcDNA3.1 expression vector by the TA-cloning system and transformation was performed on *Escherichia coli* TOP10 cells (all from Invitrogen, Carlsbad, CA). Positive transformants were analyzed for the presence and correct orientation of CD31 cDNA by polymerase chain reaction (using a combination of the T7 forward primer and of a specific reverse primer that bound to the inner sequence of CD31 cDNA) and by digestion with the *Apa*l (10 IU/μg) restriction enzyme (New England Biolabs, Beverly, MA). The selected transformant was analyzed by sequencing, grown in LB medium and purified by the Quantum Prep plasmid midiprep kit (Bio-Rad, Hercules, CA).

Transfection

Twenty μg of the CD31/pcDNA3.1 were linearized by treatment with 20 IU/μg of the *Sca*l restriction enzyme (New England Biolabs), purified, and used to stable transfect MDA-MB-231 cells by electroporation (250 V/0.4 cm and 960 μF), as described.[24] After a 2-week incubation in a medium containing 1 mg/ml of G418 (Sigma), neomycin-resistant colonies were isolated and recloned by limiting dilution. The three selected clones (namely, 2C1, 3D2, and 4B5) as well as a bulk preparation of transfected cells were referred to as MDA-MB-231 CD31$^+$. The same cell lines were similarly transfected with the empty pcDNA3.1 vector, selected using G418 and referred to as MDA-MB-231 mock-transfected cells (for short, MDA-MB-231 mock cells).

Cell Proliferation

MDA-MB-231 CD31$^+$ and control MDA-MB-231 mock cells (5×10^4 cells/ml) were seeded in 6-well plates in complete medium that was replaced every 48 hours. After 3, 4, 5, 6, and 7 days in culture, cells were detached with trypsin/ethylenediaminetetraacetic acid (Gibco BRL, Life Technologies, Paisley, Scotland) and counted by three independent observers after trypan blue dye exclusion. Fold increase was calculated as the ratio between the mean cell numbers scored and the number of cells plated at the beginning of the experiments. At least three separate experiments were performed, with the results confirmed by ^{3}H-thymidine incorporation assay [1 μCi of ^{3}H-thymidine/well (Amersham) added 8 hours before stopping the experiment], with the radioactivity measured in a β-counter.[25]

Immunophenotyping

Cells were grown on glass coverslips, rinsed twice with RPMI 1640 medium, and fixed [4% paraformaldehyde in phosphate-buffered saline (PBS) with 2% sucrose, pH 7.6] for 5 minutes, to evaluate expression of surface molecules. Intracytoplasmic proteins were visualized by exposure to ice-cold methanol (5 minutes at -20°C), followed by ice-cold acetone (5 seconds at -20°C) and air-drying. Coverslips were then washed three times with

PBS and incubated (1 hour at 37°C) with the relevant mAb. A fluorescein isothiocyanate-conjugated GαMIg was added (30 minutes at 37°C) before mounting the coverslips on slides. Analysis was performed with a C-VIEW-12-BUND camera fitted to an Olympus 1 × 70 microscope (Milano, Italy), with the images being collected using the ANALYSIS software.

As an alternative, live cells were collected from culture using ethylenediaminetetraacetic acid and conventionally stained with an indirect assay. Intensity of fluorescence was recorded on a logarithmic scale using a flow cytometer (FACSort, BD Biosciences), by scoring at least 10,000 cells/sample.

Western Blot Analysis

MDA-MB-231 cells were lysed in 1% Nonidet P-40 lysis buffer (20 mmol/L HEPES, pH 7.6, 150 mmol/L NaCl, 50 mmol/L NaF, 1 mmol/L Na_3VO_4, 1 mmol/L EGTA, 50 μmol/L phenylarsine oxide, 10 μmol/L iodoacetamide and chymostatin, leupeptin, and pepstatin) for 20 minutes on ice. After removal of nuclei by centrifugation, an aliquot of the lysates was run in sodium dodecyl sulfate-polyacrylamide gel electrophoresis (10% or 7.5%) under reducing conditions and transblotted on nitrocellulose membranes (Amersham, Little Chalfont, Buckinghamshire, UK), as described.[24] The membranes were then blocked in 5% bovine serum albumin and incubated for 1 hour with the primary antibody of interest. After washing, horseradish peroxidase-conjugated GαMIg was added and the membrane was washed and developed using enhanced chemiluminescence reagents (Amersham). Full-range rainbow molecular weight markers (Amersham) were used to determine the weight of the proteins under analysis.

Tri-Dimensional Cultures

Cells (75 × 10^3 cells/ml) were harvested from culture using trypsin-ethylenediaminetetraacetic acid, resuspended in RPMI 1640 medium plus 20% fetal calf serum and mixed with a gel matrix consisting of 1 part of RPMI 1640 medium (concentrated 10-fold), 1 part of 0.5 mol/L HEPES, pH 7.9, and 7 parts of ice-cold matrix formed by 50% bovine collagen type I (4.1 mg/ml stock solution) and 50% Matrigel basement membrane matrix (10 mg/ml stock solution, both from BD Bioscience), at a final concentration of 2.5 mg/ml. Five hundred-μl aliquots were dispensed into a preheated 24-well plate and allowed to gel (20 minutes at 37°C). One hundred μl of RPMI 1640 medium plus 20% fetal calf serum were overlaid and replaced twice a week. The plates were observed daily under a phase-contrast inverted microscope (Olympus). After 2 weeks, gels were fixed with neutral buffered formalin for 24 hours, embedded in paraffin, and stained by hematoxylin and eosin (H&E). Ducts were defined as aggregates composed of cells organized around a central lumen, as previously described.[26]

SCID Mice Experiments

MDA-MB-231 $CD31^+$ and control MDA-MB-231 mock cells (7 × 10^6) were injected monolaterally into the inguinal mammary fat pad of female SCID mice at 4 to 5 weeks of age (Charles River, Calco, Italy). Cells were resuspended in 150 μl of RPMI 1640 medium in the presence of an equal volume of Matrigel. Mice were sacrificed at 4, 5, 6, and 7 weeks after cell injection and the primary tumors, the liver, lungs, pancreas, kidneys, spleen, omentum, brain, heart, bones, skeletal muscles, uterus, and ovaries were removed, formalin-fixed, and paraffin embedded. A sample of the primary tumor was collected in sterile conditions to recultivate the cells after the period of *in vivo* growth.

Histology and Immunohistochemistry

Multiple sections of the primary tumor were deparaffinized and stained by H&E, by periodic acid-Schiff (PAS) reaction, and by trichrome stain to evaluate morphology. Multiple sections from each organ were also stained by H&E to screen for metastatic diffusion.

Sections from frozen tissues were fixed in methanol and acetone and air-dried for immunohistochemical analysis. Endogenous peroxidase of formalin-fixed paraffin-embedded tissues was inhibited by incubating (5 minutes) the specimens with 3% H_2O_2, before the incubation with the primary mAb.[27] The sections were first incubated with specific avidin- and biotin-blocking reagents (Biogenex, San Ramon, CA) when antigen retrieval was needed. Heat-induced antigen retrieval was performed by pretreatment in a microwave oven (three times for 3 minutes at 750 W) of the sections incubated in 1 mmol/L of ethylenediaminetetraacetic acid buffer, pH 8.0, or in 10 mmol/L of citrate buffer, pH 6.0. The reaction was revealed using the streptavidin-peroxidase-conjugated StrAviGen Multilink kit for 20 minutes at room temperature and developed in a solution of 3,3′-diaminobenzidine in 0.3% H_2O_2. Slides were counterstained in Mayer hemalum (all from Biogenex) for 30 seconds, dehydrated, and mounted.

Cell Migration through Matrigel

The ability of cells to migrate through Matrigel porous-coated filters was measured in a Boyden chamber (BD Biosciences) by a transwell migration assay.[28] Cells (10^5 cells/ml) were resuspended in RPMI 1640 medium plus 1% bovine serum albumin and plated in the upper part of the chamber for 24 hours, while complete medium was added as a chemoattractant in the lower part. The direct contribution of CD31 to migration was tested by adding specific blocking mAbs (ie, Moon-1, JC70, and SF4.9, final concentration of 10 μg/ml) to the upper part of the chamber, together with the cells. After incubation, the cells that had not penetrated were wiped away with cotton swabs and the cells that had migrated to the lower surface of the filter were stained with H&E, examined by bright-field microscopy, and photographed.

Comparative Analysis with Human CD31$^+$ DCIS

The tumors obtained from MDA-MB-231 CD31$^+$ cells grown in SCID mice were compared to a human sample selected as paradigmatic of a population of breast cancers recently reported.[17] The human specimen was obtained from a 63-year-old woman, who underwent quadrantectomy and sentinel lymph node biopsy in the surgical department of the local breast unit for a ductal carcinoma. The poorly differentiated invasive tumor (18-mm diameter) was associated with a DCIS of 28 mm. The patient underwent a re-excision of the lesion because foci of DCIS were on the resection margins of the surgical specimen. The second specimen also contained diffuse foci of DCIS. The morphology of the DCIS was characterized by papillary and solid growth. The cells forming the papillary structures of the DCIS were CD31$^+$, while lacking surface CD44, whereas the invasive ductal carcinoma expressed simultaneously CD31 and CD44.

Results

Establishment of CD31$^+$ Breast Cancer Cell Lines

The MDA-MB-231 CD31$^+$ cells obtained by transfection of the full-length human CD31 cDNA were used as such or subcloned by limiting dilution and constantly kept under positive selection by immunomagnetic beads and CD31 mAb separation. The *de novo* surface expression of CD31 was demonstrated on the three selected clones (namely, 2C1, 3D2, and 4B5) using cells in suspension (Figure 1A) and in adhesion to glass substrates (Figure 1B), using anti-CD31 mAbs (ie, Moon-1, JC70, and SF4.9). The presence of CD31 was further confirmed by Western blot analysis, which highlighted a single chain of ~130 kd in the three clones and in the bulk preparation of CD31$^+$ cells. Transfection with the empty pcDNA3.1 plasmid was uneventful (Figure 1, A and C). The table in Figure 1 shows that human umbilical vein endothelial cells and the three MDA-MB-231 CD31$^+$ clones display similar mean fluorescence intensity values for CD31 staining.

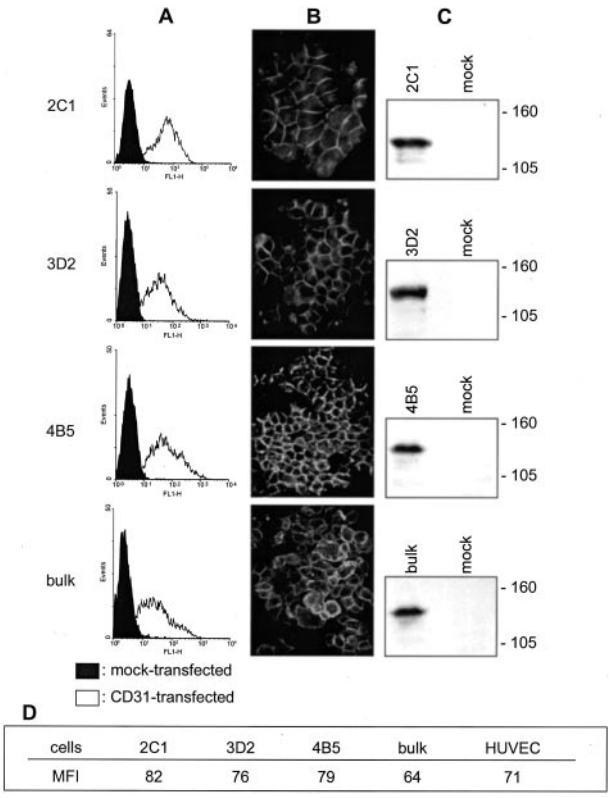

cells	2C1	3D2	4B5	bulk	HUVEC
MFI	82	76	79	64	71

Figure 1. Preparation of CD31$^+$ clones of the MDA-MB-231 cell line. Stable transfection by electroporation of a plasmid containing the full-length human CD31 gene results in the production of three MDA-MB-231 clones (2C1, 3D2, and 4B5) and a bulk preparation of cells homogeneously expressing CD31, as determined by examining cells in suspension (**A**, empty profiles) and in adherence (**B**). Western blot analysis highlights a single chain of ~130 kd in the MDA-MB-231 cells transfected with CD31 (**C**). Control MDA-MB-231 mock cells do not show detectable levels of CD31 (**A**, full panels, and **C**, mock lanes). **A:** Cells were analyzed using a FACSort equipment and scoring 10,000 events/sample. *x* axis, fluorescence intensity/cells; *y* axis, number of cells registered/channel. **B:** Cells were grown on glass coverslips, fixed using methanol and acetone, and stained. **C:** Cells were lysed using 1% Nonidet P-40, run on 10% sodium dodecyl sulfate-polyacrylamide gel electrophoresis, transblotted onto a nitrocellulose membrane, and the reactivity was examined using JC70 mAb and horseradish peroxidase-conjugated GαMIg. Molecular weight markers are indicated on the **right**. Original magnifications, ×60.

In Vitro *Effects of CD31 Expression*

Breast cancer cells *de novo* expressing CD31 were compared to the MDA-MB-231 mock cells for growth potential. Seven-day proliferation assays indicate that MDA-MB-231 CD31$^+$ cells increased approximately fourfold the number of cells seeded, as compared to the >10-fold increase of the MDA-MB-231 mock cells (Figure 2A). The trypan blue dye exclusion test confirmed that both cell lines were alive. These findings were confirmed by means of ^{3}H-thymidine incorporation tests, resulting ~40% lower in MDA-MB-231 CD31$^+$ after a 72-hour culture than in the control cell line (data not shown). Overlapping results were obtained using the three clones established as well as a bulk preparation of cells. The diminished growth ability acquired by the MDA-MB-231 CD31$^+$ cells might be secondary to qualitative and quantitative modifications of the surface molecules involved in cell-cell interactions and signal transduction. The expression of CD44 observed in MDA-MB-231 CD31$^+$ (clone 2C1, 3D2, and 4B5, and bulk cells) was significantly lower than in mock cells (Figure 2B). The diminished expression of CD44 was also confirmed using a Western blot system, which clearly showed that MDA-MB-231 CD31$^+$ cells have significantly less CD44 than mock cells (Figure 2B). The event is specific, because no modifications could be found when analyzing a selected panel of molecules expressed (ie, CD29, CD11a, and CD54 adhesion molecules, along with HLA class I and CD71), and not expressed (ie, E-cadherin and VE-cadherin) by MDA-MB-231 mock cells (data not shown).

The next step was to determine whether the phenotype modifications were followed by the acquisition of differentiation features. The marker adopted was the human milk fat globule (HMFG) protein, present in normally se-

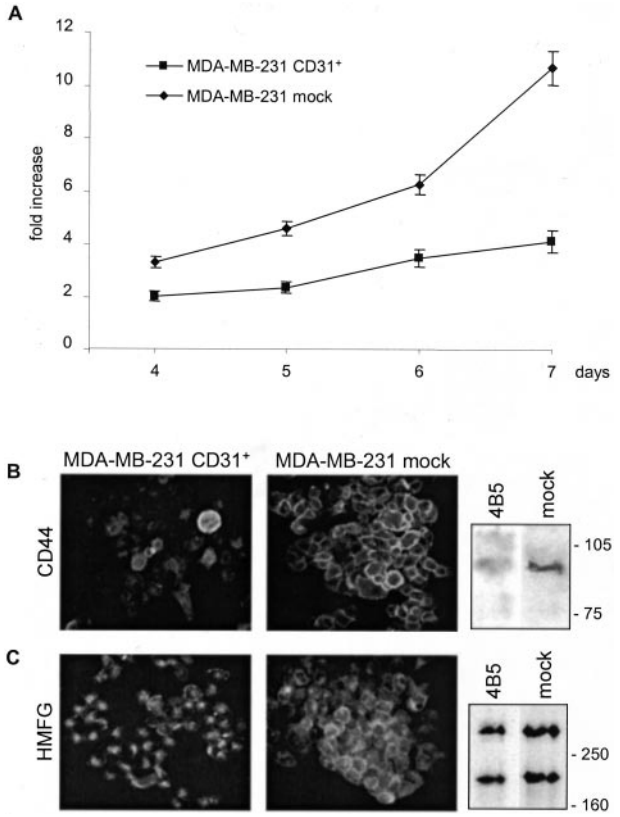

Figure 2. *In vitro* effects of CD31 transfection. CD31 transfection reduces MDA-MB-231 growth rate (**A**). MDA-MB-231 CD31$^+$ 2C1, 3D2, and 4B5 clones and mock cells were seeded in complete medium, detached, and counted after 4 to 7 days by three independent observers. Fold increase was calculated as the ratio between the mean cell numbers scored and the number of cells plated at the beginning of the experiments. Data are the mean ± SD (**vertical bars**) from four independent experiments. CD31 transfection strongly down-modulates CD44 expression (**B**, clone 4B5), as examined by immunofluorescence and Western blot analysis. Moreover, it induces cytoplasmic organization of HMFG protein in secretory vacuoles (**C**, clone 4B5). No significant differences were seen in terms of protein quantity (**C**). Cells were grown on glass coverslips, fixed, stained, and photographed. Representative images from five independent experiments obtained using three different clones as well as a bulk population of MDA-MB-231 CD31$^+$ cells. For Western blot analysis, cells were lysed using 1% Nonidet P-40, run on a 10% (CD44) or 7.5% (HMFG) sodium dodecyl sulfate-polyacrylamide gel electrophoresis, transblotted onto a nitrocellulose membrane, and the reactivity examined using JC70 mAb and horseradish peroxidase-conjugated GαMIg. Molecular weight markers are indicated on the **right**. Original magnification, ×60 (**C**).

creting breast epithelial cells and in selected carcinomas.[29] The HMFG protein is clustered in intracytoplasmic granules in MDA-MB-231 CD31$^+$ cells (clone 2C1, 3D2, and 4B5, and bulk cells), witnessing the acquisition of a secretory phenotype (Figure 2C). On the contrary, HMFG granules are scattered throughout the cytoplasm in the MDA-MB-231 mock cells. The difference in localization of the protein was not followed by significant modifications in terms of protein quantity, as evidenced in a Western blot system (Figure 2C).

Despite that conventional phase contrast microscopy of cells growing on plastic surfaces did not provide evidence for morphological changes, CD31 transfection profoundly affected the ability of cells to grow in a tridimensional modality when using collagen as a gel matrix. By day 4, ~80% of cells formed ductal-like structures

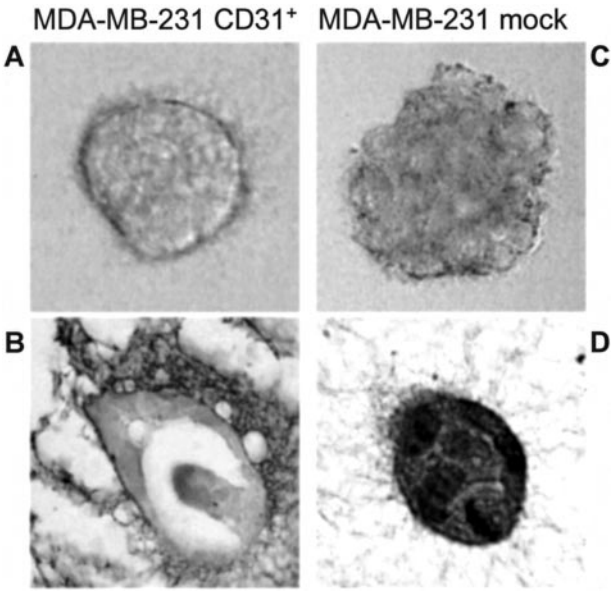

Figure 3. MDA-MB-231 CD31$^+$ cells form ductal and papillary-like structures in tri-dimensional cultures. Cells were seeded in a collagen gel matrix and observed daily by phase-contrast microscopy. After 2 weeks the gels were fixed and stained by H&E. By day 4 ~80% of MDA-MB-231 CD31$^+$ cells acquire ductal-like structures (**A**, clone 2C1), with occasional papillae growing inside the ducts (**B**, clone 2C1). Mock cells grow in a disorganized way and form solid aggregates (**C** and **D**). Original magnifications, ×100.

(Figure 3A). On the contrary, MDA-MB-231 mock cells formed colonies of simple cell clusters (Figure 3C). In addition, MDA-MB-231 CD31$^+$ cells built up intraductal structures similar to papillae inside the lumen, as observed by paraffin sections of the collagen-gel matrix cultures (Figure 3B). Paraffin sections of the collagen matrix containing MDA-MB-231 mock cells revealed solid aggregates (Figure 3D). These experiments were repeated using the three separate clones obtained and the bulk preparation of MDA-MB-231 CD31$^+$ cells.

Expansion of CD31$^+$ Breast Tumors in SCID Mice

The main question at this point was whether the events observed *in vitro* had a counterpart in an *in vivo* model, reproducing the unique growth pattern observed in human CD31$^+$ carcinomas. To this aim, MDA-MB-231 CD31$^+$ and control MDA-MB-231 mock cells were injected into the mammary fat pads of female SCID mice. The experiments were repeated using the clones 2C1, 3D2, and 4B5 separately, as well as a bulk preparation of CD31$^+$ cells. Engraftment was successful in all of the animals injected, provided that Matrigel was added to the cell suspensions.

In line with the clinical examination of the mice (Figure 4A), the tumor derived from MDA-MB-231 CD31$^+$ cells (clones 2C1, 3D2, 4B5, and bulk) were constantly and significantly smaller in size as compared to the tumors derived from mock cells (Figure 4B). At gross observation the MDA-MB-231 CD31$^+$ tumors were rubber-like solid masses, while control tumors displayed centrally colliquated necrosis. Neither set of animals had macroscopic

A

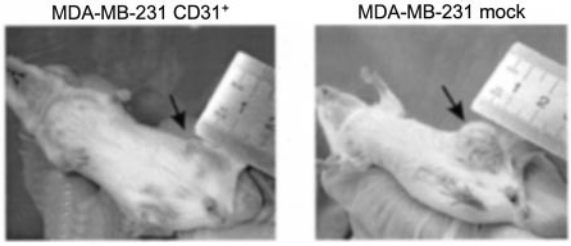

B

Weeks	2C1	3D2	4B5	bulk	mock
4	4	3.5	3.5	4.5	12 ± 2
5	5	5	4.5	5	17 ± 3
6	9.5	9	9	10	22 ± 1
7	15.25	15.5	15	16	25 ± 2

Figure 4. CD31 expression decreases growth *in vivo*. MDA-MB-231 CD31$^+$ and mock cells were injected in the mammary foot pads of female SCID mice (**arrows**) and pictures were taken after 6 weeks (**A**). The size of the lesions at different time intervals is reported in mm in the table, and the different clones are shown (**B**). Data are the mean from two animals for each clone and for the bulk preparation of CD31$^+$ cells, while they represent the mean ± SD from four animals in the MDA-MB-231 mock cells.

evidence of metastases: however, both tumors gave rise to lung and liver micrometastases after 7 weeks of *in vivo* growth.

In Vivo *Effects of CD31 Expression—Comparison with Human CD31$^+$ DCIS*

After 4 weeks *in vivo*, the MDA-MB-231 CD31$^+$ tumors histologically formed numerous small ductal structures growing within abundant hyaline stromal tissue (Figure 5A). The presence of a continuous thin layer of collagen IV, a typical marker of the integrity of the basal membrane in human DCIS, was apparent on the stromal side of the ductal structures (Figure 5C). Laminin was instead the main product of the thick hyaline intercellular stroma bundles (Figure 5E). The MDA-MB-231 mock tumors grew in solid sheets, without a detectable basal membrane or an extracellular matrix (Figure 5; B, D, and F). After 5 to 6 weeks of *in vivo* growth, the CD31$^+$ tumors showed a preferential intraductal expansion, featuring papillary-like structures similar to those observed in some CD31$^+$ human DCIS (Figure 6, A and B). The immunophenotype of CD31$^+$ tumor samples also matched that observed in CD31$^+$ human DCIS (Figure 6, D and E). The CD31 molecule was expressed at the cell membrane level, with the highest degree of positivity scored by the cells forming papillae. The basal cells lining the lumen focally expressed CD44 (Figure 6H, arrow), again in analogy to human CD31$^+$ DCIS (Figure 6G). The MDA-MB-231 mock tumors maintained the same morphology at the different time lapses (Figure 6C) as well as the phenotype of the original line, ie, CD31$^-$ and CD44$^+$, unaltered during the whole observation (Figure 6, F and I).

Several MDA-MB-231 CD31$^+$ tumor cells contained PAS-positive intracytoplasmic vacuoles (Figure 7A, arrows), a typical feature of cells producing glycoproteins. On the contrary, MDA-MB-231 mock cells were PAS-negative, while PAS outlined the stromal network (Figure 7B). MDA-MB-231 CD31$^+$ tumors actively secreted HMFG protein, which was detected in intracytoplasmic vacuoles (Figure 7C, large arrows), as seen *in vitro* (Figure 2C), and in ductal lumens formed *in vivo* (Figure 7C, small arrows). MDA-MB-231 mock cells showed scattered intracytoplasmic HMFG protein without evidence of secretion (Figure 7D, arrows).

The different growth potentials of the two lines were further witnessed by their proliferative abilities. MDA-MB-231 CD31$^+$ lesions were smaller than controls and the Ki-67 index of 1% indicates that these cells did not aggressively proliferate (Figure 7E). Conversely, the cells from MDA-MB-231 mock tumors displayed a proliferation index of 90% (Figure 7F). MDA-MB-231 CD31$^+$ cells expressed high levels of p27 (>85%), as did normal murine residual glands (Figure 7, G and H, large arrows) and normal murine stromal cells (Figure 7, G and H, small arrows). Nuclear p21 was seen in <1% of the cells and was undetectable within the cytoplasm, implying that the cells are blocked in the G_1 phase (Figure 7I). The phenotype of MDA-MB-231 mock tumors was marked by p27 in ~50% of cells (Figure 7H). Nuclear p21 was expressed in ~10% of the cells (Figure 7L, large arrows), while generalized faint cytoplasmic staining was observed in the remaining population (Figure 7L, small arrows).

Natural History of CD31$^+$ Lesions

The cells derived from tumor samples were easily reestablished in culture after the different periods of *in vivo* growth and tested for CD31 and CD44 expression. The number of MDA-MB-231 CD31$^+$ cells decreased as a function of time in all of the clones examined and in the bulk preparation of CD31$^+$ cells, resulting >90% at the time of injection, ~80% after 4 weeks, while scoring 30 to 40% after 7 weeks of *in vivo* growth. At the same time, the expression of CD44 increased from ~20% at the time of injection to >80% after 7 weeks. These findings were paralleled by the morphological modifications observed in the histological sections obtained from mice sacrificed at the same weeks. Indeed, after 7 weeks *in vivo* the MDA-MB-231 CD31$^+$ tumors displayed a mixed phenotype, with areas of intraductal papillary differentiation merging with others lacking an obvious architectural organization. These results were again comparable to those observed in patients with CD31$^+$-infiltrating carcinoma. The stroma bundles were thinner, the vascular component was reduced, and the intraluminar papillae were larger than in tumors examined at earlier times. CD31 expression was maintained at high levels by the papillary differentiated residual areas of the tumor. Collagen IV and laminin bundles were still detectable around foci of MDA-MB-231 CD31$^+$ cells (data not shown).

Effects of CD31 Expression on Tumor Motility, Diffusion, and Metastasis

The ability of MDA-MB-231 CD31$^+$ to proceed through Matrigel-coated porous filters was examined in a trans-

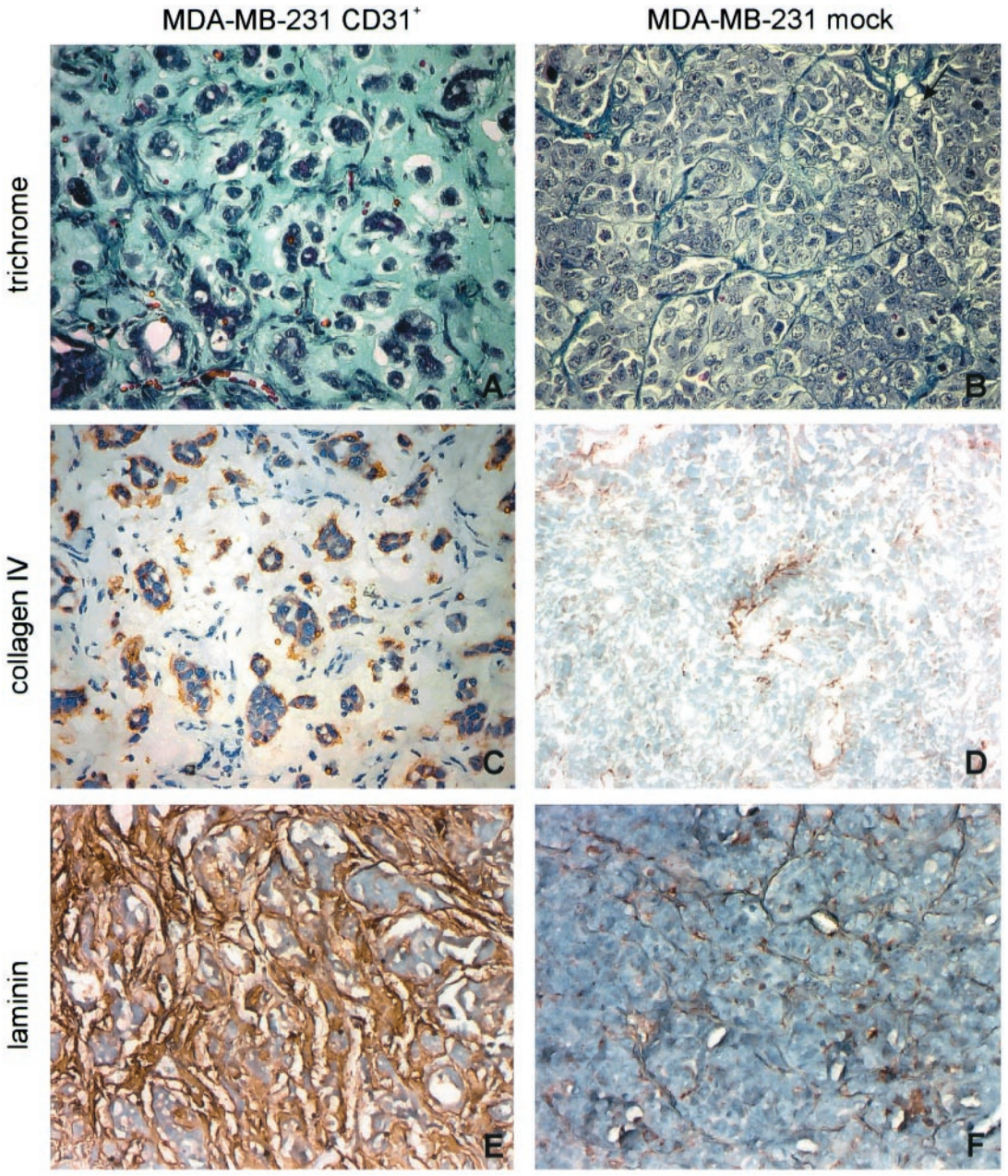

Figure 5. *In vivo* effects of CD31 expression. Histology of tumor samples derived from animals injected with MDA-MB-231 CD31$^+$ or mock cells. Trichrome stain shows that MDA-MB-231 CD31$^+$ tumors are made of cells organized in ductal structures and surrounded by thick hyaline stroma. The ducts are partly occupied by tumor cells forming papillae; blood vessels are evident (**A**). Immunohistochemistry indicates that the basal membrane of CD31$^+$ tumors is made of collagen IV (**C**) and laminin (**E**). The lesions derived from mock cells grow in solid laminae (**B**), with minimal amounts of stroma (**D** and **F**). The figure shows the histology of a tumor derived from clone 4B5. Original magnifications, ×40.

well migration assay. The number of MDA-MB-231 CD31$^+$ cells (obtained from clones 2C1, 3D2, and 4B5) migrating was significantly higher than that of mock cells. The latter were also unable to reach the lower surface of the membrane (Figure 8A, top). The migratory behavior was also reproduced by using murine L-fibroblasts expressing human CD31 instead of the mammary line (Figure 8A, bottom). The direct participation of CD31 in the migration and invasiveness acquired by the CD31$^+$ breast tumor cells was confirmed by blocking these events using anti-CD31 mAbs specific for different domains of the molecule (Figure 8B). The results obtained indicate that migration is interfered with by Moon-1, a mAb specific for CD31 domain 2, the one most involved in heterophilic interactions.[30] On the contrary, 5F4.9 and the JC70 mAbs reactive to domain 1 (responsible for homophilic interactions[31]) were only slightly effective.

The observed increased ability to migrate *in vitro* is witnessed *in vivo* by the unique tropism of MDA-MB-231 CD31$^+$ tumors for the normal ducts residual in the murine mammary gland. Murine ducts were filled with CD31$^+$ tumor cells, a feature that closely resembles the colonization of lobules and ducts that led to Paget's disease of the nipple in human CD31$^+$ DCIS. In contrast, MDA-MB-

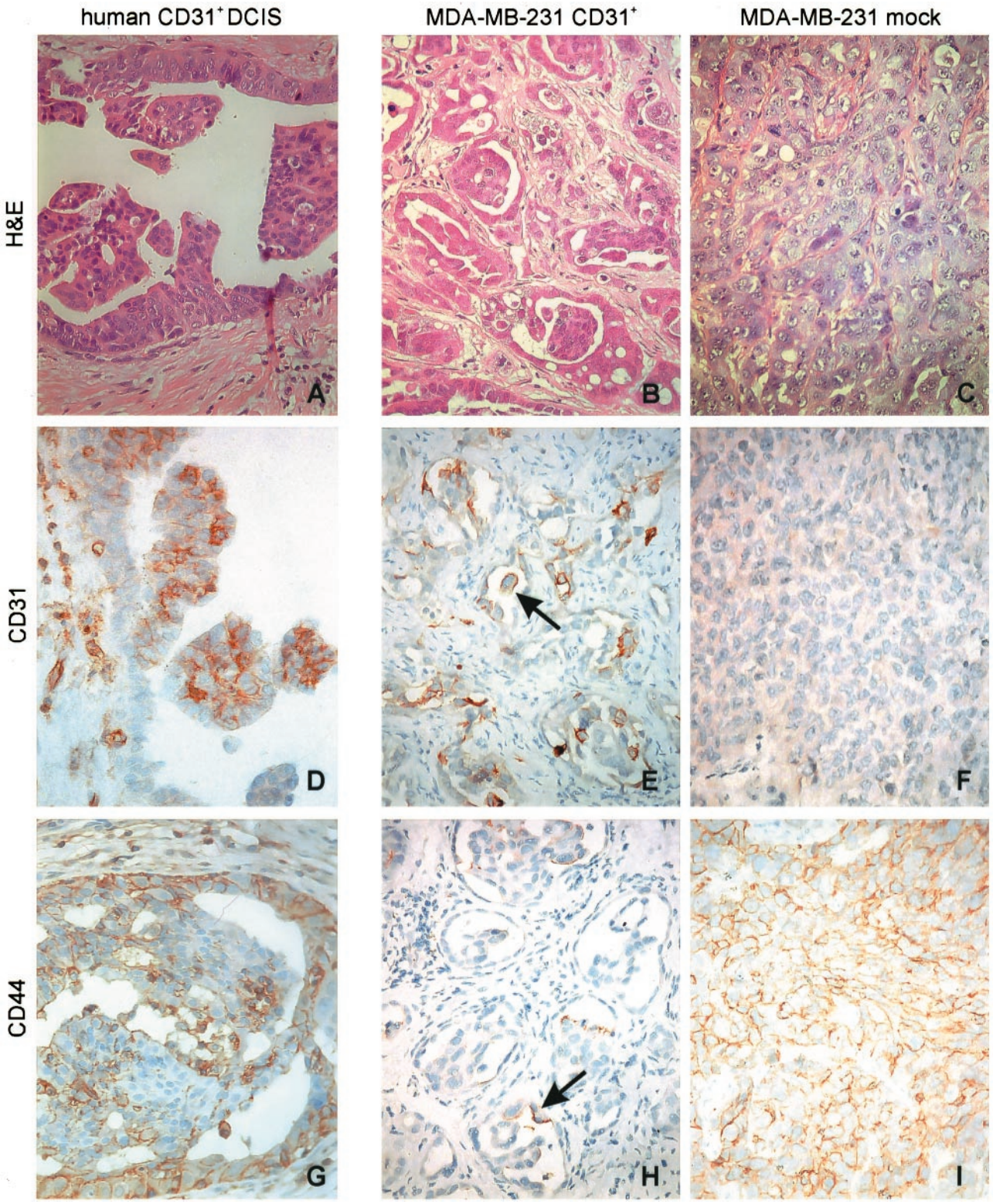

Figure 6. The tumors obtained from MDA-MB-231 $CD31^+$ cells grown in SCID mice were compared to a human sample selected as paradigmatic of a population of $CD31^+$ breast cancers. H&E staining performed after 6 weeks of growth in SCID mice shows that the MDA-MB-231 $CD31^+$ tumors preferentially expand within the ducts, forming papillae (**B**), similar to what observed in human $CD31^+$ DCIS (**A**). Conversely, MDA-MB-231 mock tumors constantly grow in solid lamina (**C**). The immunophenotype of $CD31^+$ SCID mice samples matches the one observed in human $CD31^+$ DCIS. The CD31 molecule is expressed at the cell membrane level, with the highest degree of positivity scored by the cells forming papillae (**D**, human lesions; **E**, murine lesions). The basal cells lining the lumen focally express CD44 (**H**, **arrow**), in analogy to human $CD31^+$ DCIS (**G**). MDA-MB-231 mock tumors maintained the phenotype of the original line, ie, $CD31^-$ and $CD44^+$, which was unaltered during the whole observation (**F** and **I**). The pictures were obtained from a selection of lesions derived from mice injected with MDA-MB-231 $CD31^+$ cells (clones 2C1 and 4B5). Original magnifications, ×40.

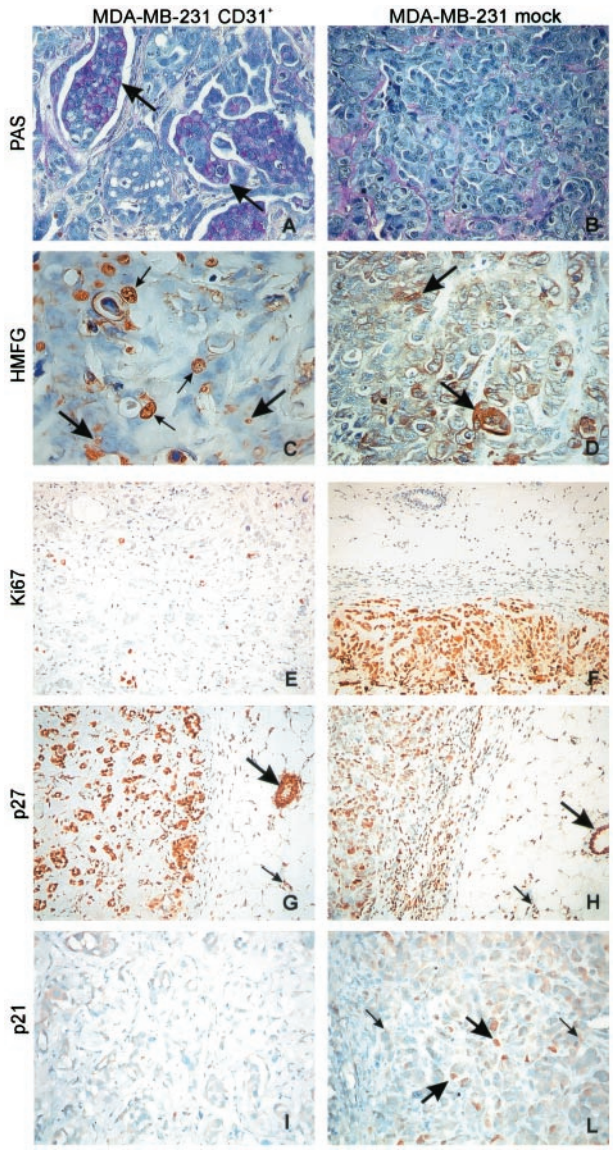

Figure 7. CD31 expression induces differentiation of MDA-MB-231 cells *in vivo.* PAS staining highlights intracytoplasmic vacuoles only in tumors derived from transfected cells and mainly in the cells forming the papillae (**A**, **arrows**; and **B**). MDA-MB-231 CD31$^+$ tumors acquire a secretory phenotype, as inferred by the presence of HMFG protein in cytoplasmic vacuoles (**large arrows**) and in some ductal lumens (**small arrows**) (**C**). Mock cells display scattered intracytoplasmic HMFG protein granules (**arrows**), without evidence of secretion (**D**). MDA-MB-231 CD31$^+$ tumor cells are not actively proliferating. Ki-67 index is <1% in MDA-MB-231 CD31$^+$ tumors (**E**), whereas p27 is highly expressed (>85%) (**G**), as are normal murine residual glands (**large arrows** in **G** and **H**) and normal stromal murine cells (**small arrows** in **G** and **H**). Conversely, mock tumors score >90% for Ki-67 (**F**) and <50% for p27 (**H**). Nuclear p21 was seen in <1% of the MDA-MB-231 CD31$^+$ cells and was undetectable within the cytoplasm, implying that the cells are blocked in the G_1 phase (**I**). MDA-MB-231 mock tumors express nuclear p21 in ~10% of the cells (**large arrows** in **L**), whereas generalized faint cytoplasmic staining was observed in the remaining population (**small arrows**). The pictures were obtained from a selection of lesions derived from mice injected with MDA-MB-231 CD31$^+$ cells (clones 2C1 and 4B5). Original magnifications: ×40 (**A–D**); ×20 (**E–L**).

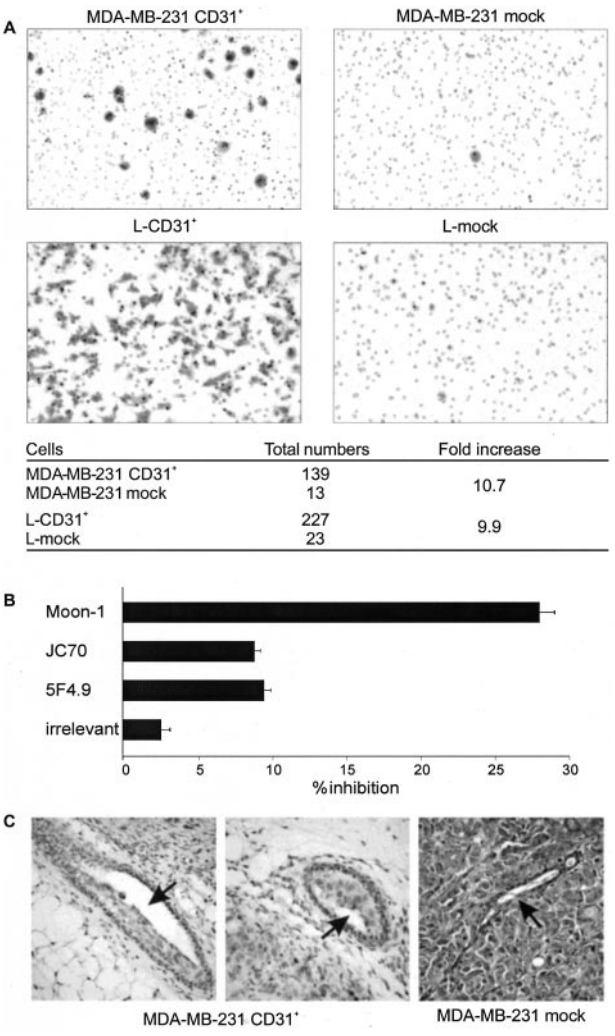

Figure 8. CD31 confers unique kinetic properties to MDA-MB-231 cells. The presence of CD31 is a prerequisite for MDA-MB-231 cells to migrate in *in vitro* assays (**A**, **top**) as well as for murine L-fibroblasts (**A**, **bottom**). The table shows cumulative data from several experiments. The **asterisks** indicate statistical significance ($P < 0.05$, Wilcoxon matched-pairs signed-ranks test). Migration is blocked only by the Moon-1 mAb (reactive to the CD31 domain 2), whereas other mAbs (reactive to the CD31 domain 1) are only slightly effective. **Vertical bars** represent the mean ± SD from four independent experiments (**B**). The unique migratory properties of MDA-MB-231 CD31$^+$ cells are characterized *in vivo* by the tendency to invade the normal murine residual mammary ducts maintaining the original architecture, as compared to the compression and destruction of the same structures evident in the lesions originated from mock cells (**C**, **arrows**; clone 4B5).

231 mock cells did not colonize the residual murine ducts, which were compressed and destroyed by the growing tumor (Figure 8C).

Animals injected with both MDA-MB-231 CD31$^+$ and mock cells developed microscopical lung metastases after 7 weeks of *in vivo* growth. No clear difference in terms of number or size could be identified among the two groups of animals, even though the analysis was intrinsically hampered by the very low number of metastases detected and the very low number of cells constituting them. However, the phenotype of the micrometastases identified in MDA-MB-231 CD31$^+$ tumors was CD44$^+$. The small dimensions of the metastatic foci limited any additional phenotyping.

Discussion

In situ growth and invasion in breast cancer are the result of a balanced equilibrium between the adhesive and

migratory properties of tumor cells and the plasticity of the surrounding milieu. The malignant behavior of a tumor depends on 1) uncontrolled growth, 2) local invasiveness, and 3) ability to metastasize. Adhesion molecules contribute to each of these features. We have evaluated the role of the adhesion receptor molecule CD31 in determining the architectural organization, differentiation, and growth of breast cancer cells. The uncommon choice of breast cancer as a model to study a molecule traditionally considered as a nonepithelial antigen stems from a previous report on the expression of CD31 by specific subsets of *in situ* and $CD44^+$ invasive carcinomas of the breast.[17] The strategy devised was to artificially express the human CD31 cDNA in the MDA-MB-231 breast cancer cell line, selected in virtue of its resemblance to the $CD31^+$ neoplastic population recently described in human breast cancer, ie, hormone independence and CD44 expression.[32] To avoid the danger of clonal variations unrelated to the transfected gene, three separate $CD31^+$ clones were isolated, characterized, and used in the experiments along with a bulk preparation of $CD31^+$-transfected cells.

The first finding is that the proliferative index of MDA-MB-231 $CD31^+$ cells was reduced by >50% after 7 days *in vitro*, an effect apparent in all of the culture conditions examined and not secondary to an increased cell death. Secondly, the high levels of surface CD31 observed after transfection were paralleled by a marked down-modulation of CD44 and by the acquisition of a differentiated secretory phenotype. This was inferred by the intracellular organization of HMFG proteins in vacuoles and from the tri-dimensional growth of MDA-MB-231 $CD31^+$ cells in ducts and papillae.

At this point the question was whether the events observed *in vitro* could have a counterpart or a validity in an *in vivo* model, reproducing the growth pattern seen in human $CD31^+$ breast lesions. The results obtained in a SCID mouse model are that the injection of MDA-MB-231 $CD31^+$ cells originated tumor masses significantly smaller than those scored by mock lesions. Secondly, the morphology of the $CD31^+$ tumors mimics that observed in human $CD31^+$ tumors. The third finding is that there is an apparently interchained expression between CD31 and CD44.

Histology and immunohistochemistry, performed on mice sacrificed at different time intervals, helped us to reconstruct a morphogenetic model for $CD31^+$ lesions. During the first weeks of *in vivo* growth, $CD31^+$ cells give rise to (or represent a hinge point for the construction of) ductal structures, which are surrounded by collagen IV and laminin, organized to delineate a real basal membrane. As observed *in vitro*, expression of CD44 at this point is very low. These histological and immunohistochemical aspects are closely reminiscent of human $CD31^+$ DCIS.[33] Next, the cells forming the ducts instead of invading the basal membrane grow inside the lumen, where they tend to accumulate and form papillae. The unique tendency of $CD31^+$ cells for rolling and piling-up[34] is visible also in the normal residual ducts of the murine mammary gland, similarly filled with accumulating $CD31^+$ cells. The migratory features mimic the intraductal diffusion of tumor cells that cause the Paget's disease of the nipple, frequently associated with human $CD31^+$ breast carcinomas. The final phase is marked by a mixed phenotype, in which the ducts and internal papillae (both $CD31^+$ and $CD44^-$) are suffocated by nests of $CD44^+$ cells. The morphological modifications observed in MDA-MB-231 $CD31^+$ tumors are accompanied by a progressive decrease of CD31 and a simultaneous increase of CD44 expressions, as shown both by immunohistochemistry and by immediate analysis of cells purified from the tumors. This phenotype is similar to what is observed in human pathology, in which$CD31^+$ DCIS cells are $CD44^-$, whereas CD31 invasive ductal carcinoma cells are $CD44^+$ and may loose CD31 expression.[17] The observation of a mutual exclusion between CD31 and CD44 may indicate a shift from the propensity to invade (conferred by the presence of CD44) to a tendency to organize (conferred by the presence of CD31). Where do the $CD31^-$ cells come from? One possibility is that the transfectants that normally lose CD31 in absence of a metabolic selection may be endowed with growth advantages, responsible for the progressive overcome of $CD31^+$ cells and for the presence of micrometastases in both groups of animals after 7 weeks *in vivo*. The size of metastases prevented accurate phenotype analyses: however, a firm conclusion is that their phenotype is $CD44^+$ in both models. An alternative possibility to explain the origin of $CD31^-$ cells is that the *in vivo* environment plays a direct role in the down-modulation of CD31, either providing a source of a soluble or surface bound counterreceptor, or as a result of a selective elimination of $CD31^+$ cells. We are currently testing the possibility that CD31 itself may be a channel for inhibitory signals, as demonstrated in other contexts.[15,35]

With some caveats, these growth modalities might be the experimental counterparts of the ones proposed for the $CD31^+$ breast cancers, primarily *in situ* carcinomas, characterized by the tendency to progress throughout the ductal structures, before becoming genuinely invasive.[17] The unique propensity of MDA-MB-231 $CD31^+$ cells to move is confirmed by the *in vitro* migration assays. Indeed, CD31 expression seems to be a prerequisite for the acquisition of kinetic properties. The same abilities are exerted by L-$CD31^+$ cells and the migration is partially blocked by specific mAbs. Moreover, the finding that only the mAbs reactive to CD31 domain 2 hamper motility suggests the existence or co-existence of heterophilic binding mechanism(s).[36]

The results obtained in this study may contrast with those obtained by the Kim and colleagues,[37] that reported that CD31 inhibits migration rates in endothelial cells. The reason for this discrepancy may be related to the use of a different cellular model (endothelial *versus* epithelial) and it is likely referable to the complex interplay taking place between CD31 and cytoskeletal proteins. This point supports the view that CD31 acts equally efficiently as an activatory or inhibitory receptor as a function of the cell type and, likely, of the microenvironment. Further attention will be devoted to the analysis of the migratory behavior in response to selected chemoat-

tractants, eg, epidermal growth factor,[38] to which MDA-MB-231 cells are known to respond.

These observations raise the possibility that CD31 plays a role in the architectural organization of breast carcinomas. According to this hypothesis, CD31 could help in establishing a polarity within mammary epithelial cells, a necessary condition for cell differentiation.[39] Evidence supporting this hypothesis comes from the ectopic expression of CD31 in transgenic mice, which affects early events of mammary gland morphogenesis, suggesting that it may regulate the ductal branching at early stages of embryogenesis.[40] Evidence against this hypothesis comes from the lack of CD31 expression by nonneoplastic human breast tissue at different stages of development.[41,42] Thus, CD31 expression in breast cancer might be the result of gene amplification, as suggested by the observation that 17q23 (the region of the chromosome where CD31 gene is localized[43]) is frequently amplified in breast carcinomas.[44] When overexpressed, CD31 may indirectly impact breast tumor morphology inducing architectural organization and blocking cell proliferation, as observed in SCID mice injected with MDA-MB-231 $CD31^+$ cells, where the cell cycle is blocked in the G_1 phase.[45]

The presence of CD31 on the membrane of malignant epithelial cells could also be explained in the context of vasculogenic mimicry.[46,47] This is an appealing theory envisaging vascular cell specialization inside a single tumor. Specific tumor elements were found to form blood-filled channels and to become intensely $CD31^+$, at least in the experimental setting of uveal melanoma.[46] Although still a topic of discussion in breast cancer[48] this model is challenging. However, in none of the $CD31^+$ murine lesions as well as of human specimens was it possible to detect the presence of red blood cells or other elements indicating a blood flow, or the expression of other surface markers associated with an endothelial cell-like phenotype (ie, F-VIII-RA and CD34).

These findings indicate that the presence of CD31 on the cell membrane is sufficient to revert the undifferentiated morphology and invasive behavior of MDA-MB-231 breast cancer cells, widening the concept of adhesion molecules from social proteins involved in cell-to-cell contacts to pleiotropic receptors ruling complex network of signals crucial in determining morphogenesis, differentiation, and diffusion of cells.

Acknowledgments

We thank H. Stockinger (Vienna, Austria) and J. Askaa (Glostrup, Denmark) for providing reagents and M. V. Dentico (Torino, Italy) for technical assistance.

References

1. DeLisser HM, Newman PJ, Albelda SM: Molecular and functional aspects of PECAM-1/CD31. Immunol Today 1994, 15:490–495
2. Muller WA, Weigl SA, Deng X, Phillips DM: PECAM-1 is required for transendothelial migration of leukocytes. J Exp Med 1993, 178:449–460
3. Muller WA, Randolph GJ: Migration of leukocytes across endothelium and beyond: molecules involved in the transmigration and fate of monocytes. J Leukoc Biol 1999, 66:698–704
4. Lu TT, Yan LG, Madri JA: Integrin engagement mediates tyrosine dephosphorylation on platelet-endothelial cell adhesion molecule 1. Proc Natl Acad Sci USA 1996, 93:11808–11813
5. Piali L, Hammel P, Uherek C, Bachmann F, Gisler RH, Dunon D, Imhof BA: CD31/PECAM-1 is a ligand for alpha v beta 3 integrin involved in adhesion of leukocytes to endothelium. J Cell Biol 1995, 130:451–460
6. Buckley CD, Doyonnas R, Newton JP, Blystone SD, Brown EJ, Watt SM, Simmons DL: Identification of alpha v beta 3 as a heterotypic ligand for CD31/PECAM-1. J Cell Sci 1996, 109:437–445
7. Treutiger CJ, Heddini A, Fernandez V, Muller WA, Wahlgren M: PECAM-1/CD31, an endothelial receptor for binding Plasmodium falciparum-infected erythrocytes. Nat Med 1997, 3:1405–1408
8. Prager E, Sunder-Plassmann R, Hansmann C, Koch C, Holter W, Knapp W, Stockinger H: Interaction of CD31 with a heterophilic counterreceptor involved in downregulation of human T cell responses. J Exp Med 1996, 184:41–50
9. Deaglio S, Morra M, Mallone R, Ausiello CM, Prager E, Garbarino G, Dianzani U, Stockinger H, Malavasi F: Human CD38 (ADP-ribosyl cyclase) is a counter-receptor of CD31, an Ig superfamily member. J Immunol 1998, 160:395–402
10. Deaglio S, Mallone R, Baj G, Arnulfo A, Surico N, Dianzani U, Mehta K, Malavasi F: CD38/CD31, a receptor/ligand system ruling adhesion and signaling in human leukocytes. Chem Immunol 2000, 75:99–120
11. Jackson DE, Ward CM, Wang R, Newman PJ: The protein-tyrosine phosphatase SHP-2 binds platelet/endothelial cell adhesion molecule-1 (PECAM-1) and forms a distinct signaling complex during platelet aggregation. Evidence for a mechanistic link between PECAM-1- and integrin-mediated cellular signaling. J Biol Chem 1997, 272:6986–6993
12. Jackson DE, Kupcho KR, Newman PJ: Characterization of phosphotyrosine binding motifs in the cytoplasmic domain of platelet/endothelial cell adhesion molecule-1 (PECAM-1) that are required for the cellular association and activation of the protein-tyrosine phosphatase, SHP-2. J Biol Chem 1997, 272:24868–24875
13. Ilan N, Mahooti S, Rimm DL, Madri JA: PECAM-1 (CD31) functions as a reservoir for and a modulator of tyrosine-phosphorylated beta-catenin. J Cell Sci 1999, 112:3005–3014
14. Ilan N, Cheung L, Pinter E, Madri JA: Platelet-endothelial cell adhesion molecule-1 (CD31), a scaffolding molecule for selected catenin family members whose binding is mediated by different tyrosine and serine/threonine phosphorylation. J Biol Chem 2000, 275:21435–21443
15. Newman DK, Hamilton C, Newman PJ: Inhibition of antigen-receptor signaling by platelet endothelial cell adhesion molecule-1 (CD31) requires functional ITIMs, SHP-2, and p56(lck). Blood 2001, 97:2351–2357
16. Newton-Nash DK, Newman PJ: A new role for platelet-endothelial cell adhesion molecule-1 (CD31): inhibition of TCR-mediated signal transduction. J Immunol 1999, 163:682–688
17. Sapino A, Bongiovanni M, Cassoni P, Righi L, Arisio R, Deaglio S, Malavasi F: Expression of CD31 by cells of extensive ductal in situ and invasive carcinomas of the breast. J Pathol 2001, 194:254–261
18. Kremmidiotis G: CD44. J Biol Regul Homeost Agents 1999, 13:234–239
19. Cailleau R, Young R, Olive M, Reeves Jr WJ: Breast tumor cell lines from pleural effusions. J Natl Cancer Inst 1974, 53:661–674
20. Deaglio S, Dianzani U, Horenstein AL, Fernandez JE, van Kooten C, Bragardo M, Funaro A, Garbarino G, Di Virgilio F, Banchereau J, Malavasi F: Human CD38 ligand. A 120-KDA protein predominantly expressed on endothelial cells. J Immunol 1996, 156:727–734
21. Baj G, Arnulfo A, Deaglio S, Tibaldi E, Surico N, Malavasi F: All-trans retinoic acid inhibits the growth of breast cancer cells by up-regulating ICAM-1 expression. J Biol Regul Homeost Agents 1999, 13:115–122
22. Deaglio S, Canella D, Baj G, Arnulfo A, Waxman S, Malavasi F: Evidence of an immunologic mechanism behind the therapeutical effects of arsenic trioxide (As(2)O(3)) on myeloma cells. Leuk Res 2001, 25:227–235
23. Deaglio S, Capobianco A, Cali A, Bellora F, Alberti F, Righi L, Sapino A, Camaschella C, Malavasi F: Structural, functional and tissue distribution analyses of the human transferrin receptor-2 molecule by

means of murine monoclonal and polyclonal antibodies. Blood 2002, 100:3782–3789
24. Deaglio S, Zubiaur M, Gregorini A, Bottarel F, Ausiello CM, Dianzani U, Sancho J, Malavasi F: Human CD38 and CD16 are functionally dependent and physically associated in natural killer cells. Blood 2002, 99:2490–2498
25. Baj G, Arnulfo A, Deaglio S, Mallone R, Vigone A, De Cesaris MG, Surico N, Malavasi F, Ferrero E: Arsenic trioxide and breast cancer: analysis of the apoptotic, differentiative and immunomodulatory effects. Breast Cancer Res Treat 2002, 73:61–73
26. Yang J, Richards J, Bowman P, Guzman R, Enami J, McCormick K, Hamamoto S, Pitelka D, Nandi S: Sustained growth and three-dimensional organization of primary mammary tumor epithelial cells embedded in collagen gels. Proc Natl Acad Sci USA 1979, 76:3401–3405
27. Bussolati G, Gugliotta P, Volante M, Pace M, Papotti M: Retrieved endogenous biotin: a novel marker and a potential pitfall in diagnostic immunohistochemistry. Histopathology 1997, 31:400–407
28. Albini A, Iwamoto Y, Kleinman HK, Martin GR, Aaronson SA, Kozlowski JM, McEwan RN: A rapid in vitro assay for quantitating the invasive potential of tumor cells. Cancer Res 1987, 47:3239–3245
29. Taylor-Papadimitriou J, Peterson JA, Arklie J, Burchell J, Ceriani RL, Bodmer WF: Monoclonal antibodies to epithelium-specific components of the human milk fat globule membrane: production and reaction with cells in culture. Int J Cancer 1981, 28:17–21
30. Liao F, Huynh HK, Eiroa A, Greene T, Polizzi E, Muller WA: Migration of monocytes across endothelium and passage through extracellular matrix involve separate molecular domains of PECAM-1. J Exp Med 1995, 182:1337–1343
31. Nakada MT, Amin K, Christofidou-Solomidou M, O'Brien CD, Sun J, Gurubhagavatula I, Heavner GA, Taylor AH, Paddock C, Sun QH, Zehnder JL, Newman PJ, Albelda SM, DeLisser HM: Antibodies against the first Ig-like domain of human platelet endothelial cell adhesion molecule-1 (PECAM-1) that inhibit PECAM-1-dependent homophilic adhesion block in vivo neutrophil recruitment. J Immunol 2000, 164:452–462
32. Hardwick M, Rone J, Han Z, Haddad B, Papadopoulos V: Peripheral-type benzodiazepine receptor levels correlate with the ability of human breast cancer MDA-MB-231 cell line to grow in SCID mice. Int J Cancer 2001, 94:322–327
33. Bose S, Derosa CM, Ozzello L: Immunostaining of type IV collagen and smooth muscle actin as an aid in the diagnosis of breast lesions. Breast J 1999, 5:194–201
34. Sun J, Paddock C, Shubert J, Zhang HB, Arnin K, Newman PJ, Albelda SM: Contributions of the extracellular and cytoplasmic domains of platelet-endothelial cell adhesion molecule-1 (PECAM-1/CD31) in regulating cell-cell localization. J Cell Sci 2000, 113:1459–1469
35. Brown S, Heinisch I, Ross E, Shaw K, Buckley CD, Savill J: Apoptosis disables CD31-mediated cell detachment from phagocytes promoting binding and engulfment. Nature 2002, 418:200–203
36. Muller WA, Berman ME, Newman PJ, DeLisser HM, Albelda SM: A heterophilic adhesion mechanism for platelet/endothelial cell adhesion molecule 1 (CD31). J Exp Med 1992, 175:1401–1404
37. Kim CS, Wang T, Madri JA: Platelet endothelial cell adhesion molecule-1 expression modulates endothelial cell migration in vitro. Lab Invest 1998, 78:583–590
38. Price JT, Tiganis T, Agarwal A, Djakiew D, Thompson EW: Epidermal growth factor promotes MDA-MB-231 breast cancer cell migration through a phosphatidylinositol 3′-kinase and phospholipase C-dependent mechanism. Cancer Res 1999, 59:5475–5478
39. Streuli CH, Schmidhauser C, Bailey N, Yurchenco P, Skubitz AP, Roskelley C, Bissell MJ: Laminin mediates tissue-specific gene expression in mammary epithelia. J Cell Biol 1995, 129:591–603
40. Ilan N, Cheung L, Miller S, Mohsenin A, Tucker A, Madri JA: Pecam-1 is a modulator of stat family member phosphorylation and localization: lessons from a transgenic mouse. Dev Biol 2001, 232: 219–232
41. Damjanovich L, Fulop B, Adany R, Nemes Z: Integrin expression on normal and neoplastic human breast epithelium. Acta Chir Hung 1997, 36:69–71
42. Anbazhagan R, Bartkova J, Stamp G, Pignatelli M, Gusterson B, Bartek J: Expression of integrin subunits in the human infant breast correlates with morphogenesis and differentiation. J Pathol 1995, 176:227–232
43. Xie Y, Muller WA: Assignment of PECAM1 to human chromosome bands 17q22->q23 by in situ hybridization. Cytogenet Cell Genet 1996, 74:156
44. Monni O, Barlund M, Mousses S, Kononen J, Sauter G, Heiskanen M, Paavola P, Avela K, Chen Y, Bittner ML, Kallioniemi A: Comprehensive copy number and gene expression profiling of the 17q23 amplicon in human breast cancer. Proc Natl Acad Sci USA 2001, 98:5711–5716
45. Wong SC, Chan JK, Lee KC, Hsiao WL: Differential expression of p16/p21/p27 and cyclin D1/D3, and their relationships to cell proliferation, apoptosis, and tumour progression in invasive ductal carcinoma of the breast. J Pathol 2001, 194:35–42
46. Maniotis AJ, Folberg R, Hess A, Seftor EA, Gardner LM, Pe'er J, Trent JM, Meltzer PS, Hendrix MJ: Vascular channel formation by human melanoma cells in vivo and in vitro: vasculogenic mimicry. Am J Pathol 1999, 155:739–752
47. Hendrix MJ, Seftor EA, Meltzer PS, Gardner LM, Hess AR, Kirschmann DA, Schatteman GC, Seftor RE: Expression and functional significance of VE-cadherin in aggressive human melanoma cells: role in vasculogenic mimicry. Proc Natl Acad Sci USA 2001, 98: 8018–8023
48. Shirakawa K, Wakasugi H, Heike Y, Watanabe I, Yamada S, Saito K, Konishi F: Vasculogenic mimicry and pseudo-comedo formation in breast cancer. Int J Cancer 2002, 99:821–828